Femtosecond laser additive manufacturing of iron and tungsten parts

Bai Nie, Lihmei Yang, Huan Huang, Shuang Bai, Peng Wan & Jian Liu

Applied Physics A
Materials Science & Processing

ISSN 0947-8396

Appl. Phys. A
DOI 10.1007/s00339-015-9070-y

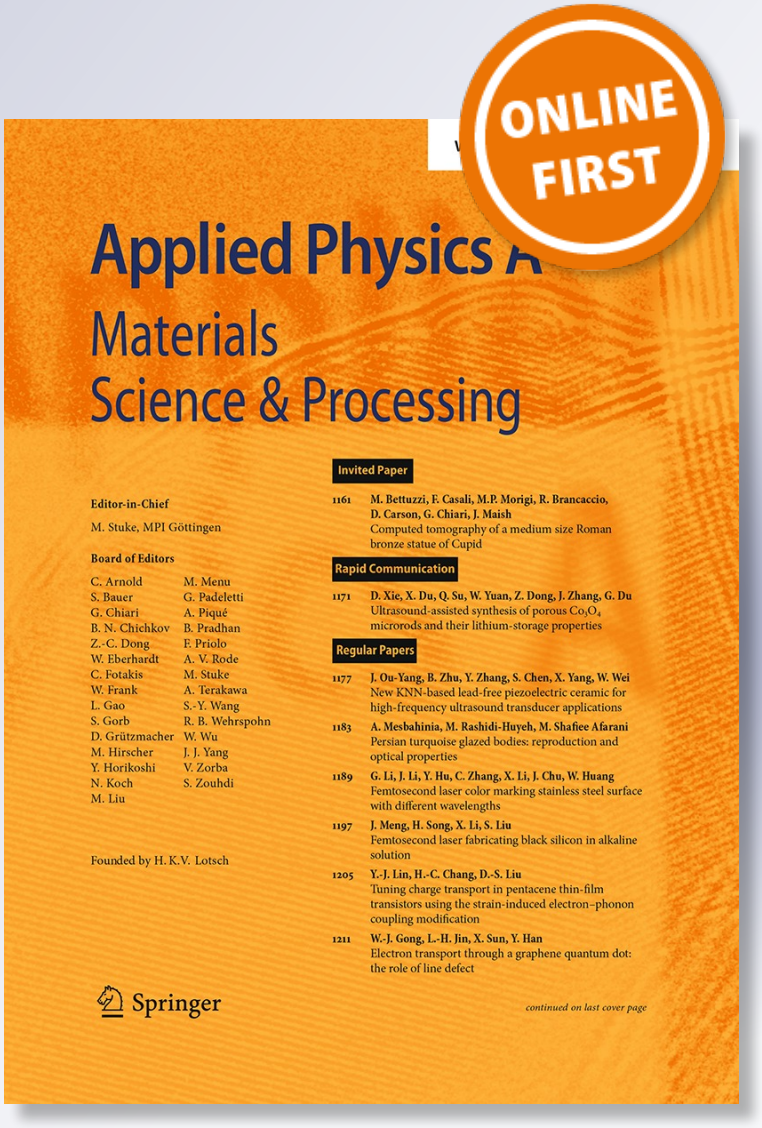

Springer

Appl. Phys. A
DOI 10.1007/s00339-015-9070-y

Applied Physics A
Materials Science & Processing

Femtosecond laser additive manufacturing of iron and tungsten parts

Bai Nie · Lihmei Yang · Huan Huang · Shuang Bai · Peng Wan · Jian Liu

Received: 22 December 2014 / Accepted: 19 February 2015

Abstract For the first time, femtosecond laser additive manufacturing is demonstrated. Pure iron and tungsten powders, having very different melting temperature and mechanical properties, are used for the demonstration. Parts with various shapes, such as ring and cube, are fabricated. Micro-hardness and ultimate tensile strength are investigated for the fabricated samples. The results are also compared to the similar parts made by a continuous-wave laser. It is found that fs laser additive manufacturing can obtain better mechanical properties and fabricate materials that are not possible before.

1 Introduction

Additive manufacturing (AM), especially laser-aided AM, has attracted lots of attentions in the past two decades [1, 2]. Laser AM of metal parts is among the most intensively studied in recent years [3, 4]. Currently, high-power continuous-wave (CW) lasers are widely used, along with some long pulsed lasers (nanosecond to millisecond pulse duration) [4, 5]. Though many breakthroughs have been achieved, there are still many challenges to overcome, such as lack of accuracy due to the large heat-affected zone, and limited type of materials [6]. In particular, for high temperature (>3000 °C) material with large thermal conductivity (>100 $W(mK)^{-1}$), like tungsten [7] and some ceramics [8], extremely high power will be needed to achieve full melting of the samples. This is not practical.

B. Nie (✉) · L. Yang · H. Huang · S. Bai · P. Wan · J. Liu
PolarOnyx, Inc., 2526 Qume Drive, Suites 17 & 18, San Jose, CA 95131, USA
e-mail: bnie@polaronyx.com

Ultrafast lasers are attracting more attentions and have many significant applications in various fields, such as material processing [9], spectroscopy [10], and biomedical imaging [11]. The extreme short pulse duration and exceptional high peak power make it unique compared to other laser sources. Advantages like high resolution and accuracy, less heat-affected zone [9], and extremely high-temperature generation (>7000 °C) [12, 13], provide fs lasers unique opportunity to play an unprecedented role in additive manufacture. Recently, we reported, for the first time, fs fiber laser is used to melt materials with extremely high melting temperature [14]. In that study, single layer of powders was used to demonstrate the feasibility of full melting of high-temperature materials like tungsten (melting temperature 3422 °C), rhenium (3182 °C) and some ultrahigh-temperature ceramics (>3000 °C). That demonstration showed a great promise of adopting fs fiber lasers in AM.

In this work, we extended our research to multi-layer melting or shaped parts. Various shaped parts (rings and cubes) were fabricated by fs fiber lasers, for the first time. Iron and tungsten powders were used for the tests. Mechanical properties and micro-structure of the fabricated parts were investigated in details. Similar parts made by CW laser were also analyzed for comparison.

2 Experimental setup

In our experiments, two types of lasers—femtosecond and CW—were used. They are 1-MHz repetition rate fs Yb fiber laser (Uranus-mJ, PolarOnyx laser, Inc., California), 80-MHz repetition rate fs Yb fiber laser (Uranus, PolarOnyx laser, Inc., California), and continuous-wave Yb fiber laser. All of the lasers have a central wavelength of

Published online: 03 March 2015

1030 nm. The 1-MHz and 80-MHz lasers have the full width half maximum (FWHM) pulse duration of 400 and 350 fs, respectively. A home-built selective laser melting setup was used for the test (Fig. 1). The laser beam was guided through an acoustic-optical modulator (AOM), which was used to control the laser on/off and variation of the laser power. A laser scanner, equipped with an F-theta lens (100 mm long focal length), was synchronized with the AOM and used to scan the laser beam on the powder surface. The scanner was mounted on a motorized stage to control the focal condition of the laser beam relative to the powder surface. The powders were evenly distributed on a substrate with a blade. The sample container was mounted on a z stage and filled with argon gas to prevent oxidation. After one layer of powder was scanned, the sample container was lowered by a certain distance and a new layer of powders was recoated onto it using the blade. The new powder surface remained the same level as the previous one.

Two materials were tested here, iron powders (1–5 microns, Atlantic Equipment Engineering, New Jersey) and tungsten powders (1–5 microns, Atlantic Equipment Engineering, New Jersey). Their melting points are 1538 and 3422 °C, respectively. For both materials, 0.9-mm-thick 304 stainless steel plates were used as the substrates. Parts with the shape like ring and cube were fabricated. The experiment parameters, such as scanning speed and focal condition, were varied for different materials or lasers. The processed samples were analyzed with the grain structures, micro-hardness (Buehler Micromet 2004) and ultimate tensile strength (Nanovea-YLD141216-8-P, Irvine, CA).

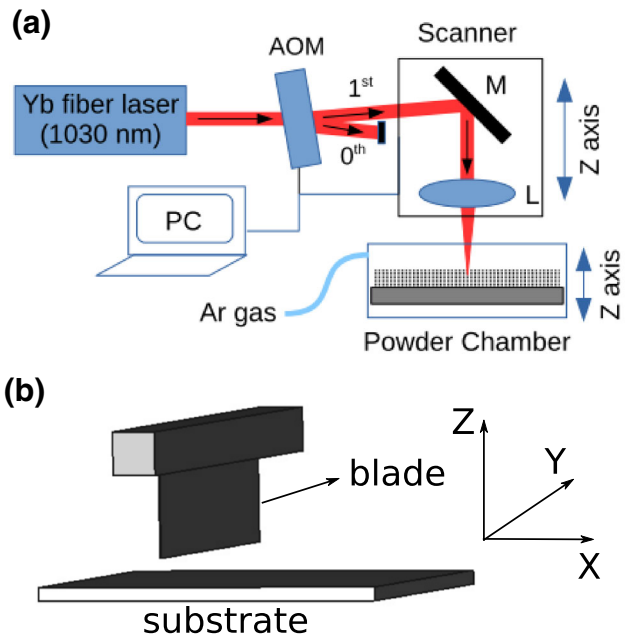

Fig. 1 Sketch of experimental setup. **a** Parts and layout of experimental setup. *AOM* acoustic-optical modulator, *M* galvanic mirrors, *L* lens. **b** Sketch of powder bed setup

3 Results and discussion

3.1 Iron powders

Iron rings with thin walls were fabricated with both 80-MHz fs and CW lasers. For both lasers, the powder surface was located at the focal plane of the scanning lens to achieve the maximum amount of melting. Without powder on the substrate, single lines were scanned on the substrate with various speeds (10, 50, 100 mm/s) to find the proper parameters for laser melting. The scanning speed of 50 mm/s was chosen for both of the lasers. All the processing parameters, such as laser power, scan speed, and focal condition, were kept the same for these two lasers during the process. Both lasers were controlled to deliver average powers of 50 W. On each layer, a single circle of 4 mm radius was scanned. In total, 40 layers of powders were melted. Each layer had a thickness about 25 microns.

The samples were cut along the direction perpendicular to the substrate plate. The obtained cross sections were imaged by high-magnification microscope. As seen in Fig. 2, the CW-fabricated iron ring showed worse continuity compared to the 80-MHz laser sample. It is also noticed that the penetration depth to the substrate was about 30 ± 5 μm for the 80-MHz laser-fabricated sample, compared to 75 ± 7 μm of the CW laser-fabricated sample, see Fig. 2. This shallower penetration is due to the less heat-affected zone, which is one of the most important characteristics of fs laser material processing [9]. This also resulted in a different thickness of each melted layer. With the same number of powder layers, the total height of the 80-MHz and CW laser-fabricated sample was about 0.9 ± 0.1 mm and 1.1 ± 0.1 mm, respectively (Fig. 3). The wall

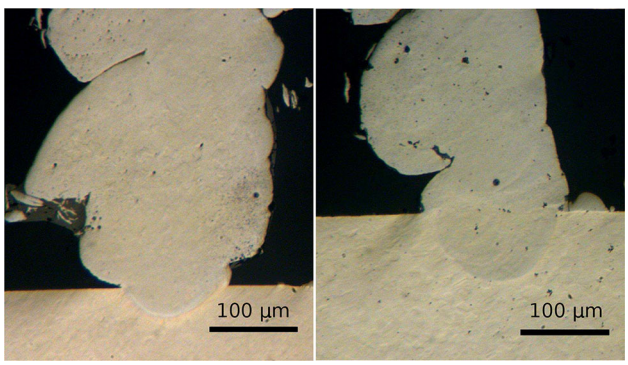

Fig. 2 Cross sections of the iron rings made by 80-MHz laser (*left*) and CW laser (*right*)

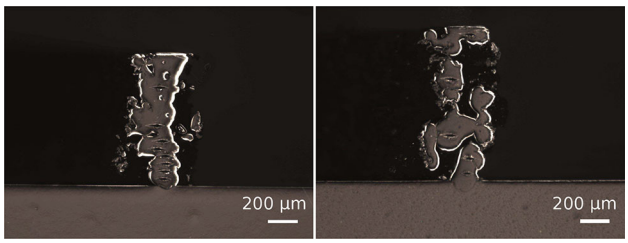

Fig. 3 Full images of the cross sections after micro-hardness tests. *Left* 80-MHz fs fiber laser-processed sample; *Right* CW laser-processed sample

thickness was around 300 and 380 μm, respectively (Fig. 3). Such different penetration depth may also affect the mechanical property of the fabricated samples. The energy-dispersive X-ray spectroscopy (IXRF 500) was conducted on both cross sections and the as-polished top surfaces, which shows very similar results with little oxidation for both samples.

Micro-hardness measurement was taken on the cross sections of both samples, from near the substrate to the top part. The dependence of hardness on sample positions was investigated. A load of 200 g and 10 s dwell time was used for the measurement of the micro-hardness. Both Knoop hardness and Rockwell hardness were given by the measurement device. As shown in Table 1, for both samples, the closer to the substrate, the softer the material is. At similar locations, the 80-MHz laser-fabricated sample is always much harder than the CW-fabricated sample. The stainless steel substrate was also tested and had an average Knoop hardness of 183.3. Most parts of the 80-MHz fabricated sample were even harder than the stainless steel 304.

In order to understand the variation of the hardness, the cross sections were etched for micro-structure analysis, see Fig. 4. The average grain size was determined by the ASTM (American Society for Testing Materials) Standard E112. For both samples, it was found that the average grain size became larger as it moved further away from the substrate. For 80-MHz laser-fabricated sample, the average grain size is about ASTM #5.5 (52 μm) near the top and #9.5 (13.5 μm) near the substrate. For CW laser-fabricated sample, the grain size is about ASTM #5 (62 μm) near the top and #9 (16 μm) near the substrate. The fine grain size near the bottom was the result of grain refinement, as the heat flow during the multi-layer melting was from top to bottom [15]. Normally, the hardness is inversely proportional to the grain size. Therefore, the parts near the bottom of our samples are harder than those near the top. However, our results showed opposite trends in both samples. In our case, we think that the residual heat from the next layer caused the re-crystallization of the previous layer due to the very thin layer thickness (about 20 μm). Though the re-crystallization resulted in smaller grain size, the residual stress was also released and caused the lower hardness. Compared with the CW-fabricated sample, the grain size of the 80-MHz laser-fabricated sample is smaller, which explains the overall larger hardness of the 80-MHz laser-processed sample. The slightly larger grain size for CW-fabricated samples is probably due to the lower cooling rate from CW laser melting and larger heat-affected zone [15]. In order to learn more about this, more studies with variation of layer thickness and other parameters are required.

The 1-MHz fs fiber laser, with maximum average power 45 W (45 μJ pulse energy), was also used for making iron sample. The corresponding pulse energy was 45 μJ. Due to the high peak power of this laser, different scanning parameter was used. For the 1-MHz laser, the maximum amount of melting of the substrate was achieved when the surface was about 2 mm below the laser focus, at the scan speed of 100 mm/s. This focal condition was chosen for the following experiments using the 1-MHz laser. Faster scan speed was used to avoid excessive ablation. A much thinner wall (220 μm) was obtained (Fig. 5). Less penetration depth to the substrate was found compared to the previously discussed two samples. The cross section of the sample was also analyzed for the micro-hardness and grain structure. A similar trend was found as the previous two samples. However, the average grain size is ASTM #7 near the substrate and ASTM #5 near the top. Though the

Table 1 Results of micro-hardness measurements on the iron rings fabricated by the 80-MHz and CW lasers

80-MHz laser sample			CW laser sample		
Distance from substrate (mm)	Knoop Hardness	HRB	Distance from substrate (mm)	Knoop Hardness	HRB
0.04	167.3	81.1	0.05	138.0	69.5
0.14	171.8	82.6	0.15	149.0	74.6
0.24	222.8	94.2	0.30	140.7	70.8
0.65	233	96.4	0.70	198.2	89.4
Average	198.7	88.6	Average	156.5	76.1

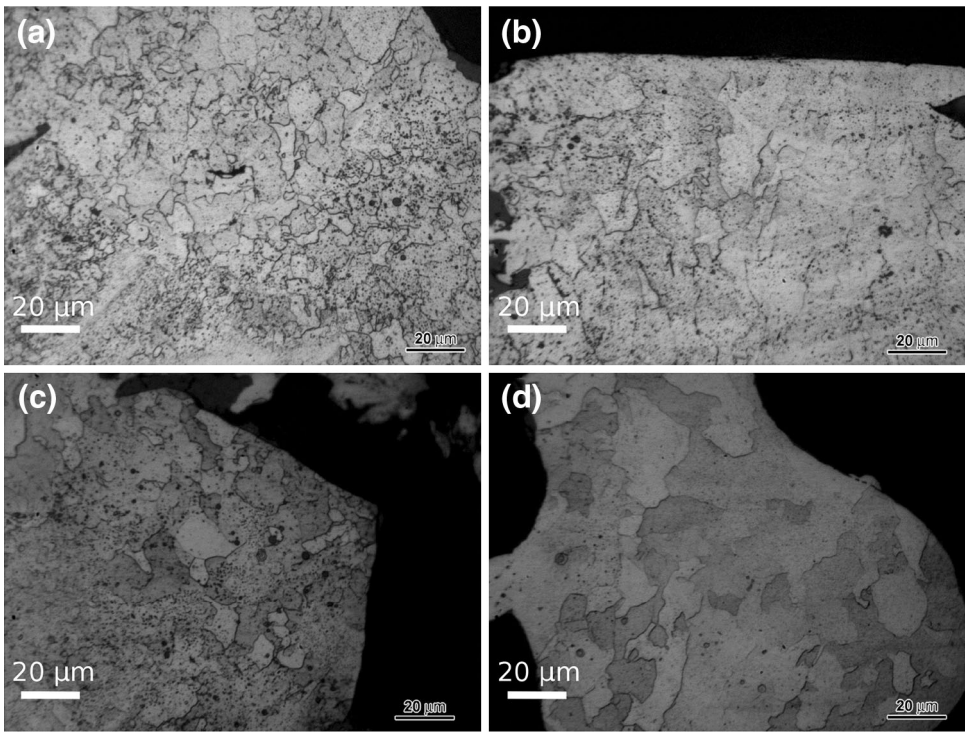

Fig. 4 *Top row*, the grain structure of the 80-MHz laser-fabricated sample, **a** near the substrate and **b** near the top. *Bottom row*, the grain structure of the CW laser-fabricated sample, **c** near the substrate and **d** near the top

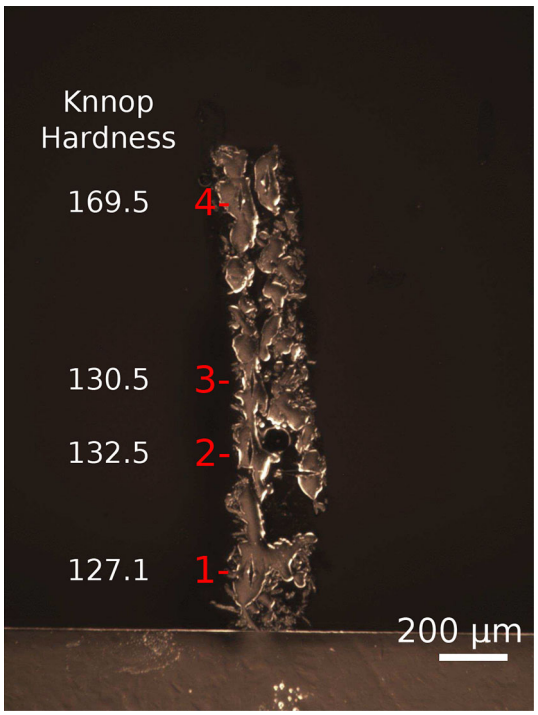

Fig. 5 Cross section image of the 1-MHz fs laser-fabricated iron sample

grain size was comparable to the previous two samples, a lower hardness (varying from 127 to 169, Knoop hardness) was measured on this sample. We are still investigating why the overall grain size is larger and material is softer.

3.2 Tungsten powders

Based on the tests of iron powders and melting of tungsten powders [14], we believe that manufacturing of shaped parts with fs lasers is feasible. This leads us to test the more challenging material—tungsten. Tungsten has the highest melting temperature (3422 °C) among all the element and very high thermal conductivity [173 $W(mK)^{-1}$], which is very challenging for current laser melting techniques.

Here, all three lasers mentioned above were used for the test. We extended the sample size to a cube in order to measure the ultimate tensile strength. Due to the much higher melting temperature compared with the iron, slower scan speed was used for tungsten melting. According to our previous study, 25 mm/s is a proper scan speed for this test. Here, stainless steel 304 plate was still used as the substrate. Though 80-MHz laser and CW laser had higher average power (50 W), it is difficult to create strong bonding between the tungsten powder and the substrate. This is due to the insufficient temperature generated to completely melt both parts. While using 1-MHz laser (average power 45 W), a solid tungsten cube was fabricated and strongly attached to the substrate.

The position of the powder surface relative to the focal plane of the scanner lens was adjusted throughout the process to achieve the best melting result. In the first few layers, the powder surface is close to the focus in order to create strong bonding between tungsten and the substrate. With more layers were deposited, the powder surface was

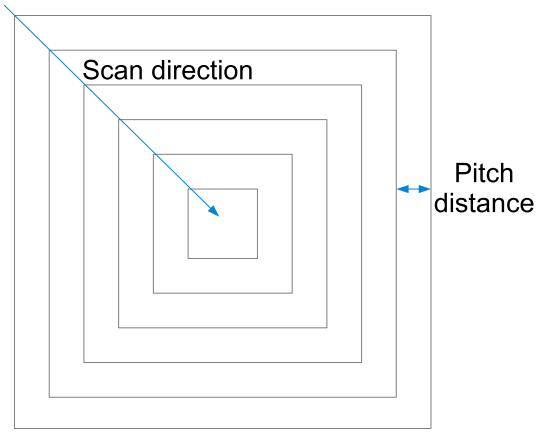

Fig. 6 Scanning scheme for each layer of the tungsten melting

moved away from the focus to reduce the peak intensity and make a smoother layer. The scanning scheme for each layer is illustrated in Fig. 6. Multiple square loops with reduced outline diameter were used to cover the full area (5 mm × 5 mm). Pitch distance of 200 µm was experimentally found to be a good parameter and was used for the test. Each layer of new powder was deposited by lowering the sample surface 15 µm. More than 100 layers of each sample were melted. The pictures of the fabricated samples are shown in Fig. 7. We found that little oxidation was observed for tungsten samples, as tungsten can be very easily oxidized [16].

Ultimate tensile strength (UTS) was measured by a tensile tester (Nanovea-YLD141216-8-P) with ASTM E3546 standard. The fabricated sample was mounted through an epoxy buck. Both the top and bottom surfaces were directly contact with the measurement device to ensure accurate measurement. A 200 µm diameter flat circular tip was pressed on the top surface with gradually increasing force (80 N/min) up to 38 N, corresponding to a pressure of 1.2 GPa. Then, the applied force was unloaded with a rate of 80 N/min. The corresponding indentation was recorded, see Fig. 8. The UTS was determined by the computer program associated with the measurement device. An average ultimate tensile strength of 388.4 ± 10.1 MPa was obtained from three sites measurement. This is much higher than the conventionally sintered tungsten parts that have an ultimate tensile strength around 18,000 psi (125 MPa) [17]. Commercially pure coarse grain tungsten parts are very brittle and fractured with a stress level less than 500 MPa [18]. The polycrystalline tungsten rods at room temperature commonly have the UTS around 580–1470 MPa [7]. In order to significantly improve tungsten's UTS, post-processing such as cold work hardening is normally required to obtain ultrafine grains [7, 17, 19]. The UTS of our sample is already much higher than the conventionally sinter parts. There are two main factors—porosity and oxidation—limiting the UTS of our sample. It is known that the ductility of tungsten is very sensitive to most of the impurities [7]. We believe that the UTS of our tungsten parts can be greatly improved by optimizing our processing setup and parameters. Better process chamber with lower oxygen level is required for the future study.

Micro-hardness measurement was also taken on the sample top surface with 300 g load and 10 s dwell time. Several locations across the top surface were measured, and no obvious variation of the results was observed. It gave an average Knoop hardness 404.3 (HRC 40.2), corresponding to Vickers hardness 395. This value is comparable to the Vickers hardness of the polycrystalline tungsten 450 and higher than the recrystallized tungsten 300 [7]. Further improvement of the hardness will be studied by varying the processing parameters.

4 Conclusion

For the first time, we have demonstrated the fabrication of shaped parts with two very different powder materials using fs fiber lasers, 80- and 1-MHz repetition rate. Iron rings and tungsten cube were fabricated and investigated for their mechanical properties and grain structures. A CW laser was also used to process the same materials for comparison. With similar average powder, these three lasers showed very different results due to their very different peak powers. It was shown that 80-MHz repetition fs laser achieved the best results for iron sample in terms of shape and mechanical properties. Only 1-MHz repetition fs

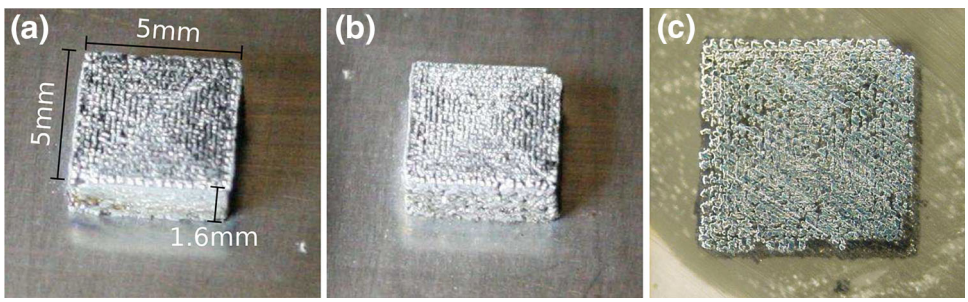

Fig. 7 Pictures of the tungsten cube manufactured by 1-MHz fs laser. **a**, **b** Pictures of tungsten cube on the substrate from different angle of views; **c** polished top surface of the tungsten cube

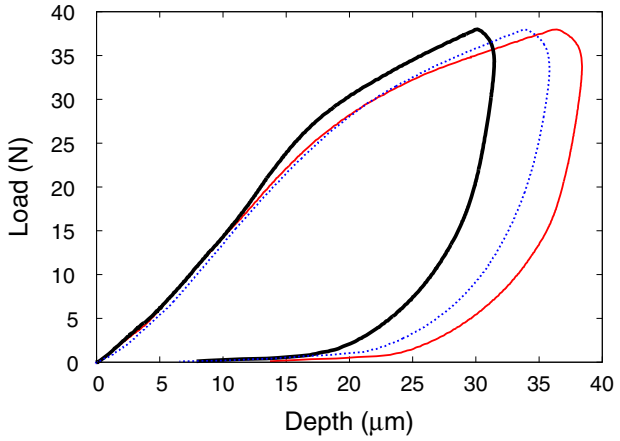

Fig. 8 UTS measurement. Indentation depth versus loading force. *Three curves* represent three separate measurements

laser was able to make a solid tungsten cube. Though 80-MHz and CW laser had higher average power, they were unable to completely melt and bond tungsten to the substrate. It is believed that the high peak power of 1-MHz laser played the key role in the melting of tungsten. This finding is very important for fabricating high-temperature materials. Although discontinuity and porosity were observed in the fabricated parts, which require further optimization of the processing parameters, we believe that this demonstration marks a great milestone toward manufacturing more complex parts with fs lasers. This will benefit automobile, aerospace, and biomedical industries that demand products of high-temperature materials with superior mechanical properties and accuracy.

References

1. J.P. Kruth, CIRP Ann. Manuf. Technol. **40**(2), 603 (1991)
2. I. Gibson, D.W. Rosen, B. Stucker, *Additive Manufacturing Technologies* (Springer, New York, 2010)
3. G.K. Lewis, E. Schlienger, Mater. Des. **21**(4), 417 (2000)
4. J.P. Kruth, L. Froyen, J. Van Vaerenbergh, P. Mercelis, M. Rombouts, B. Lauwers, J. Mater. Process. Technol. **149**(1), 616 (2004)
5. F. Abe, K. Osakada, M. Shiomi, K. Uematsu, M. Matsumoto, J. Mater. Process. Technol. **111**(1), 210 (2001)
6. W. Yeong, C. Yap, M. Mapar, C. Chua, in *High Value Manufacturing: Advanced Research in Virtual and Rapid Prototyping: Proceedings of the 6th International Conference on Advanced Research in Virtual and Rapid Prototyping*, Leiria, Portugal, 1–5 October, 2013 (CRC Press, 2013), p. 65
7. E. Lassner, W.D. Schubert, *Tungsten: Properties, Chemistry, Technology of the Elements, Alloys, and Chemical Compounds* (Springer, New York, 1999)
8. J.M. Lonergan, W.G. Fahrenholtz, G.E. Hilmas, J. Am. Ceram. Soc. **97**(6), 1689–1691 (2014)
9. B. Chichkov, C. Momma, S. Nolte, F. Von Alvensleben, A. Tünnermann, Appl. Phys. A **63**(2), 109 (1996)
10. H. Huang, L.M. Yang, J. Liu, *SPIE Defense, Security, and Sensing* (International Society for Optics and Photonics, San Francisco, 2012)
11. W.R. Zipfel, R.M. Williams, W.W. Webb, Nature Biotechnol. **21**(11), 1369 (2003)
12. S. Eaton, H. Zhang, P. Herman, F. Yoshino, L. Shah, J. Bovatsek, A. Arai, Opt. Express **13**(12), 4708 (2005)
13. R. Weber, T. Graf, P. Berger, V. Onuseit, M. Wiedenmann, C. Freitag, A. Feuer, Opt. Express **22**(9), 11312 (2014)
14. B. Nie, H. Huang, S. Bai, J. Liu, Appl. Phys. A **118**(1), 37–41 (2015)
15. B. Song, S. Dong, S. Deng, H. Liao, C. Coddet, Opt. Laser Technol. **56**, 451 (2014)
16. A.C. Reardon, *Metallurgy for the Non-metallurgist* (ASM International, Geauga, 2011)
17. F.F. Schmidt, H.R. Ogden, *The Engineering Properties of Tungsten and Tungsten Alloys* (Technical report, DTIC Document, 1963)
18. Q. Wei, T. Jiao, K. Ramesh, E. Ma, L. Kecskes, L. Magness, R. Dowding, V. Kazykhanov, R. Valiev, Acta Mater. **54**(1), 77 (2006)
19. Q. Wei, L. Kecskes, Mater. Sci. Eng. A **491**(1), 62 (2008)